J|A|C|S
ARTICLES
Published on Web 02/27/2002

A Noncovalent Approach to Antiparallel β-Sheet Formation

Huaqiang Zeng,[†] Xiaowu Yang,[†] Robert A. Flowers, II,[§] and Bing Gong*,[†]

Contribution from the Department of Chemistry, Natural Sciences Complex, State University of New York, Buffalo, New York 14260, and Department of Chemistry and Biochemistry, Texas Tech University, Box 41061, Lubbock, Texas 79409-1061.

Received March 16, 2001

Abstract: Four tripeptide chains, when attached to the same end of a hydrogen-bonded duplex (**1·2**) with the unsymmetrical, complementary sequences of ADAA/DADD, have been brought into proximity, leading to the formation of four hybrid duplexes, **1a·2a**, **1a·2b**, **1b·2a**, and **1b·2b**, each of which contains a two-stranded β-sheet segment. The extended conformations of the peptide chains were confirmed by 1D and 2D NMR. The peptide strands stay registered through hydrogen bonding and the β-sheets are stabilized by side chain interactions. Two-dimensional NMR data also indicate that the duplex template prevents further aggregation in the peptide segment. When the peptide chains are attached to the two different termini of the duplex template, NMR studies show the presence of a mixture with no clearly defined conformations. In the absence of the duplex template, the tripeptides are found to associate randomly. Finally, isothermal titration calorimetry studies revealed that the hybrid duplex **1a·2a** was more stable than either the duplex template or the peptides alone.

Introduction

Understanding β-sheet formation is critical to many problems and applications involving protein folding and design. Discerning the factors affecting β-sheet structure and stability may eventually lead to novel peptide antibiotics,[1−3] and to treatments for diseases in which β-sheet formation plays a key role.[4,5] Although as common as the α-helical structure in proteins, the β-sheet secondary structure is not well understood due to the lack of well-defined β-sheets amenable to detailed biophysical evaluation. Current efforts in developing model systems of β-sheets are focused on the design of short peptides that fold in solutions.[6−17] Artificial systems consisting of β-strands linked by unnatural templates have also been described.[18−20] The stability of the resulting β-hairpins and related model structures is found to depend on hydrogen bonding, side chain interactions, and the types of β-turns and turn mimetics. We report here the nucleation of antiparallel β-sheet-like structures based on a noncovalent, self-assembling approach.

We recently described hydrogen-bonded duplexes based on linear oligoamide strands bearing arrays of hydrogen-bonded donors (D) and acceptors (A).[21−24] These molecular duplexes are formed by pairing two single strands of complementary hydrogen-bonding sequences. The formation of these duplexes is highly sequence-specific: a single strand only pairs with another strand of its complementary sequence. Due to the absence of secondary electrostatic interactions[25−27] in this system, the stability of a duplex is sequence-independent and is proportional to the number of H-bonds found in that duplex. Both the H-bonding sequences and the number of H-bonding sites in a duplex are easily adjustable. Since the single strands of the H-bonded duplexes adopt an extended conformation similar to that of β-strands, these single strands can be regarded as β-strand mimics and the corresponding duplexes as two-stranded β-sheet mimics. Indeed, the interstrand distance of a

* Address correspondence to this author. E-mail: bgong@chem.buffalo.edu.
[†] State University of New York.
[§] Texas Tech University.

(1) Hancock, R. E. W.; Chapple, D. S. *Antimicrob. Agents. Chemother.* **1999**, *43*, 1317.
(2) Lehrer, R. I.; Ganz, T. *Curr. Opin. Immunol.* **1999**, *11*, 23.
(3) Lansbury, P. T., Jr. *Acc. Chem. Res.* **1996**, *29*, 317.
(4) Kelly, J. W. *Curr. Opin. Struct. Biol.* **1998**, *8*, 101.
(5) Soto, C. *J. Mol. Med.-JMM* **1999**, *77*, 412.
(6) Smith, C. K.; Regan, L. *Acc. Chem. Res.* **1997**, *30*, 153.
(7) Gellman, S. H. *Curr. Opin. Chem. Biol.* **1998**, *2*, 717.
(8) Lacroix, E.; Kortemme, T.; de la Paz, M. L.; Serrano, L. *Curr. Opin. Struct. Biol.* **1999**, *9*, 487.
(9) Espinosa, J. F.; Gellman, S. H. *Angew. Chem., Int. Ed.* **2000**, *39*, 2330.
(10) Griffiths-Jones, S. R.; Searle, M. S. *J. Am. Chem. Soc.* **2000**, *122*, 8350.
(11) Russell, S. J.; Cochran, A. G *J. Am. Chem. Soc.* **2000**, *122*, 12600.
(12) Pozdnyakova, I.; Guidry, J.; Wittung-Stafshede, P. *J. Am. Chem. Soc.* **2000**, *122*, 6337.
(13) Koide, S.; Huang, X. L.; Link, K.; Koide, A.; Bu, Z. M.; Engelman, D. M. *Nature* **2000**, *403*, 456.
(14) De Alba, E.; Santoro, J.; Rico, M.; Jimenez, M. A. *Protein Sci.* **1999**, *8*, 854.
(15) Schenck, H. L.; Gellman, S. H. *J. Am. Chem. Soc.* **1998**, *120*, 4869.
(16) Kortemme, T.; Ramirez-Alvarado, M.; Serrano, L. *Science* **1998**, *281*, 253.
(17) Das, C.; Raghothama, S.; Balaram, P. *J. Am. Chem. Soc.* **1998**, *120*, 5812.
(18) Nowick, J. S. *Acc. Chem. Res.* **1999**, *32*, 287.
(19) Chitnumsub, P.; Fiori, W. R.; Lashuel, H. A.; Diaz, H.; Kelly, J. W. *Bioorg. Med. Chem.* **1999**, *7*, 39.
(20) (a) Nowick, J. S.; Abdi, M.; Bellamo, K. A.; Love, J. A.; Martinez, E. J.; Noronha, G.; Smith, E. M.; Ziller, J. W. *J. Am. Chem. Soc.* **1995**, *117*, 89. (b) Holmes, D. L.; Smith, E. M.; Nowick, J. S. *J. Am. Chem. Soc.* **1997**, *119*, 9, 7665−7669.
(21) Gong, B. *Synlett* **2001**, *5*, 582.
(22) Zeng, H.; Ickes, H.; Flowers, R. A., II; Gong, B. *J. Org. Chem.* **2001**, *66*, 3574.
(23) Zeng, H.; Miller, R.; Flowers, B., II; Gong, B. *J. Am. Chem. Soc.* **2000**, *122*, 2635.
(24) Gong, B.; Yan, Y.; Zeng, H.; Skrzypczak-Jankunn, E.; Kim, Y. W.; Zhu, J.; Ickes, H. *J. Am. Chem. Soc.* **1999**, *121*, 5607.
(25) Pranata, J.; Wierschke, S. G.; Jorgensen, W. L. *J. Am. Chem. Soc.* **1991**, *113*, 2810−2819.
(26) Jorgensen, W. L.; Pranata, J. *J. Am. Chem. Soc.* **1990**, *112*, 2008−2010.
(27) Murray, T. J.; Zimmerman, S. C. *J. Am. Chem. Soc.* **1992**, *114*, 4010−4011.

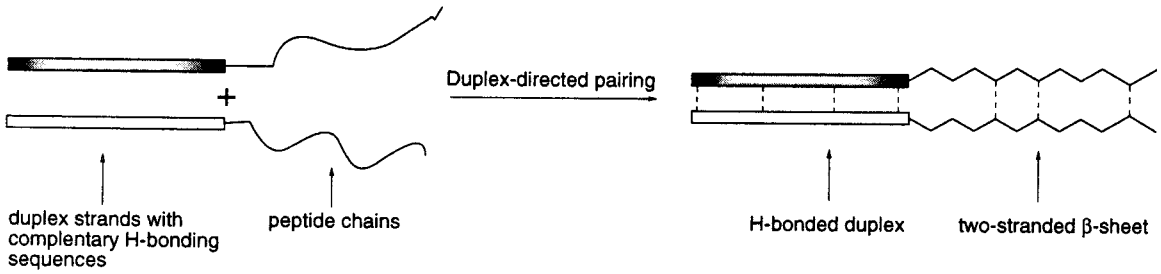

Figure 1. When attached to a duplex template, two otherwise flexible peptide chains may be directed to form a stably folded β-sheet.

duplex is nearly the same as that between two natural β-strands.[24] Therefore, these hydrogen-bonded duplexes may serve as a set of specific, noncovalent templates for the nucleation of β-sheet structures when attached to natural oligopeptides (Figure 1). The stability of the resultant hybrid structure should be enhanced if there is cooperativity along the strand direction.[14]

To evaluate this strategy, we designed four hybrid single strands **1a**, **1b**, **2a**, and **2b**, each consisting of a template segment and a natural tripeptide chain. The template is based on the quadruply hydrogen-bonded duplex **1·2,** which contains the unsymmetrical, complementary H-bonding sequences ADAA/DADD. The template-directed pairing of **1a** with **2a** and **2b**, and **1b** with **2a** and **2b**, may lead to four different hybrid duplexes **1a·2a**, **1a·2b**, **1b·2a**, and **1b·2b**. Three closely related questions need to be addressed: First, will the unsymmetrical duplex template regiospecifically bring the peptide chains into proximity? Second, will the templated peptide strands pair with each other? Third, can the paired peptide strands adopt a double-stranded, antiparallel β-sheet conformation? The amino acid residues of the tripeptides are chosen based on (1) facilitating assignment of NMR spectra, (2) propensity for β-sheet formation, and (3) our finding that the amino acid residues directly attached to the duplex templates need to be glycine.[28]

To test whether the template can indeed direct the assembly of the peptide chains in a regiospecific way, hybrid single strand **1c** was designed by attaching a tripeptide chain to the "wrong" end of **1**. As controls, the hybrid duplexes **1c·2a** and **1c·2b**, formed by pairing single strand **1c** with **2a** and **2b**, should not be able to have a β-sheet segment because the peptide chains are attached to the two different termini of the duplex template. Tripeptides **3**, **4a**, and **4b** are also included for comparison with the above hybrid strands and duplexes.

Results and Discussion

Synthesis. The synthesis is based on standard amide/peptide coupling chemistry.[29]

Characterization of the Hybrid Duplexes Containing Tripeptide Segments. The solubility of the 1:1 mixtures of single strands **1a** and **2a**, **1a** and **2b**, **1b** and **2a**, and **1b** and **2b** in $CHCl_3$ provided initial evidence for the formation of the corresponding duplexes. These 1:1 mixtures of single strands completely dissolved into $CHCl_3$ and led to stable solutions (>6 mM at room temperature). On the other hand, single strands **1a**, **1b**, and **1c** were less soluble in $CHCl_3$ (<4 mM at room temperature), and single strands **2a** and **2b** (<0.5 mM at room temperature) precipitated out upon cooling from 60 °C to room temperature.

(28) Unpublished data.
(29) For NMR spectra, synthetic procedures, other details, and analysis, see the Supporting Information.

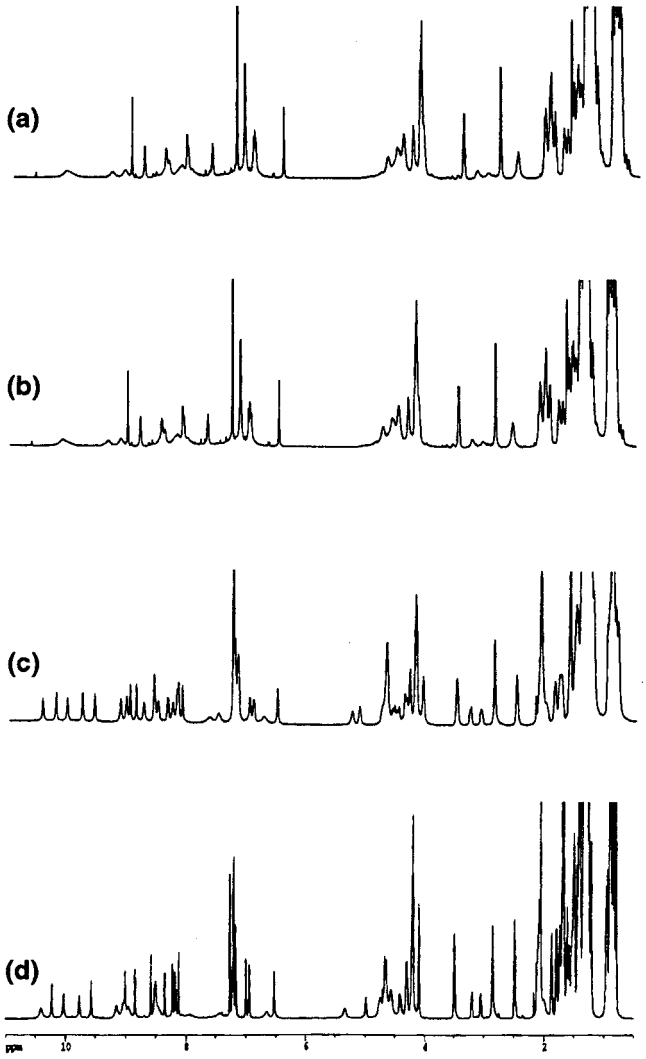

Figure 2. The ^{1}H NMR spectra of the 1:1 mixtures of (a) **1c** + **2a**, (b) **1c** + **2b**, (c) **1a** + **2b**, and (d) **1a** + **2a**.

(1) One-Dimensional (1D) ^{1}H NMR Spectroscopy. As shown in Figure 2**,** each of the 1D ^{1}H NMR spectra of duplexes **1a·2a** and **1a·2b** contains a set of sharp resonances that are indicative of well-defined conformational species in solution. The presence of sharp amide NH signals between 9.50 and 10.50 ppm is consistent with the existence of strong intermolecular H-bonds. Similarly, duplexes **1b·2a** and **1b·2b** also give spectra with sharp, well-defined peaks that are similar to those of **1a·2a** and **1a·2b**.[29] In contrast, the 1D ^{1}H NMR spectra of **1c·2a** and **1c·2b** contain broad, poorly defined resonances, indicating slowly equilibrating mixtures with multiple associating modes.

The H_α chemical shifts of duplexes **1a·2a** and **1a·2b** are compared with those of duplexes **1c·2a** and **1c·2b**, single strands

Chart 1

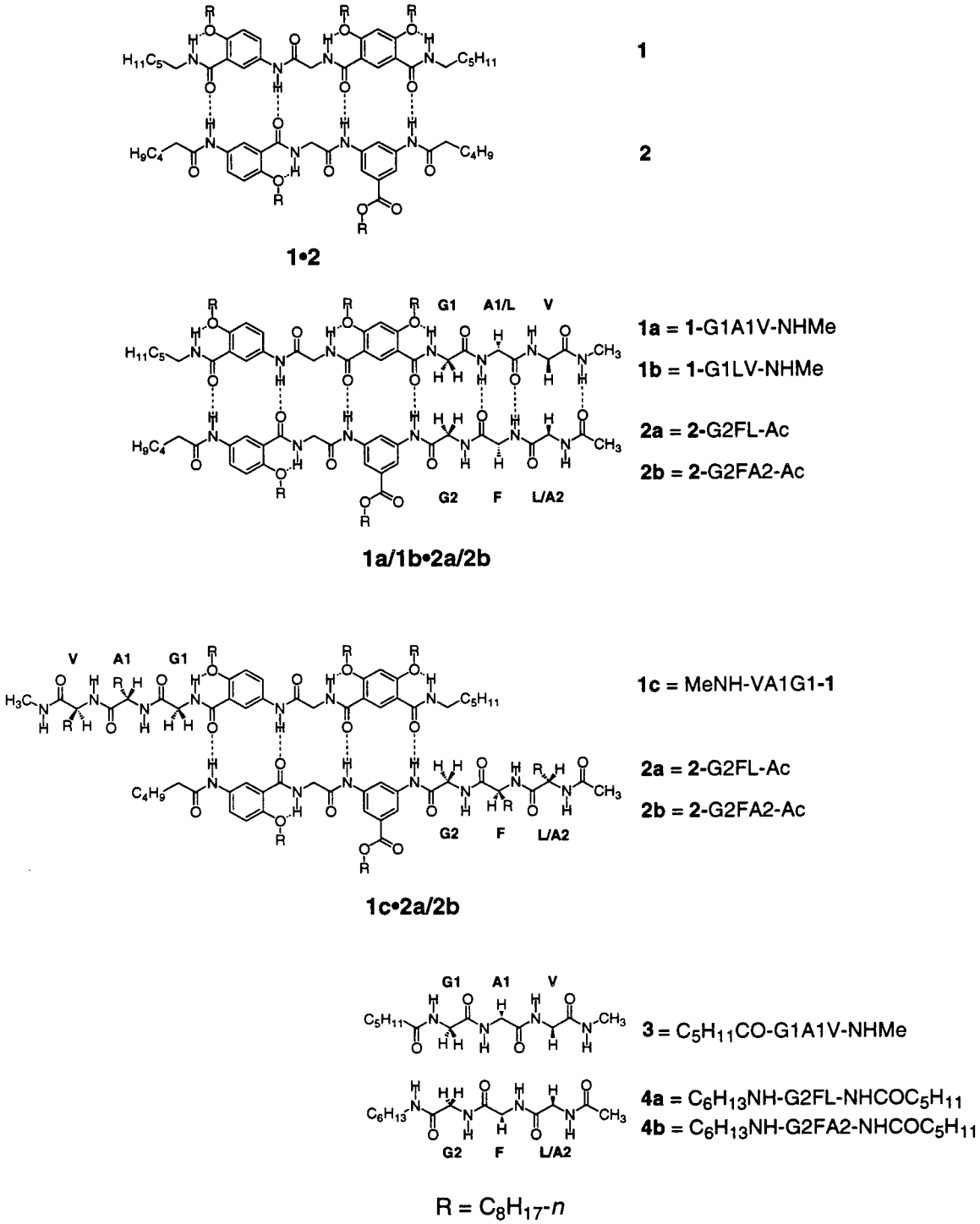

1a and **1c**, tripeptides **4a** and **4b**, and 1:1 mixtures of tripeptides **3** and **4a**, and **3** and **4b**. The results are listed in Table 1. Significant differences exist between the H_α chemical shifts of **1a·2a** and **1a·2b** and those of the others (Table 1). Most of the H_α signals in **1a·2a** and **1a·2b** are shifted downfield as compared to those of the single hybrid strands, the tripeptides, and **1c·2a** and **1c·2b** whose peptide segments are not likely to be paired. These data suggest that the α-protons in duplexes **1a·2a** and **1a·2b** are placed in a unique structural environment. The observed changes of the H_α chemical shifts of **1a·2a** and **1a·2b** are most likely the result of interstrand interactions in β-sheet-like structures.[30]

(2) Two-Dimensional ^{1}H NMR Spectroscopy.[29] Two-dimensional (2D) NMR (NOESY, 500 and 800 MHz, 4 mM in $CDCl_3$) studies were carried out on duplexes **1a·2a**, **1a·2b**, **1b·2a**, and **1b·2b**. Numerous interstrand NOEs corresponding to the template regions of all four duplexes were observed. These contacts include those between protons *1* and *42*, *1* and *41*, *4* and *41*, *6* and *40*, *10* and *36*, *10* and *35*, and *10* and *33* (Figure 3). These NOEs indicate that the template strands are sequence-specifically registered in the expected unsymmetrical fashion, a prerequisite for the correct pairing of the two tripeptides

(30) Maynard, A. J.; Sharman, G. J.; Searle, M. S. *J. Am. Chem. Soc*. **1998**, *120*, 1996.

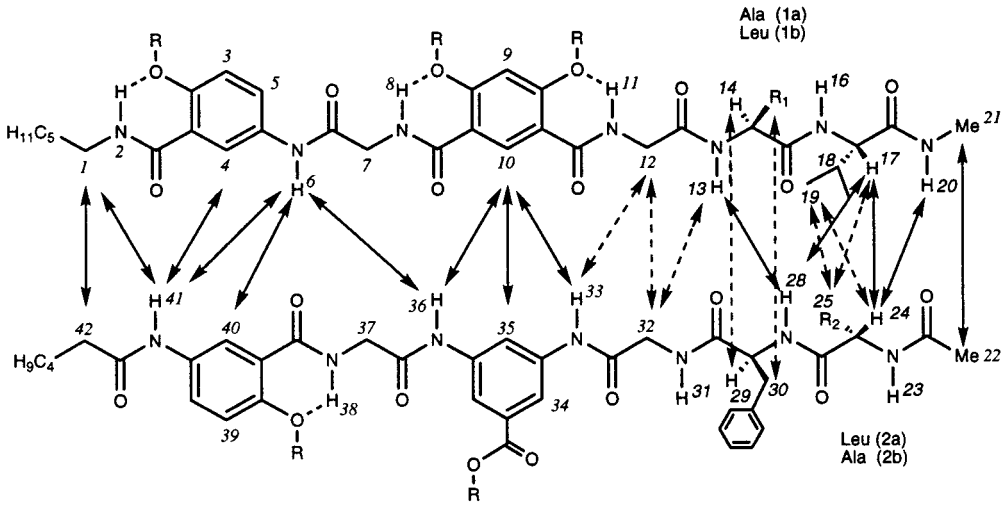

1a/1b•2a/2b (R = -C_8H_{17}-*n*)

Figure 3. Summary of cross-strand NOEs (NOESY, 500 MHz, mixing time 0.5 s, 4 mM in $CDCl_3$) observed for the four hybrid duplexes **1a·2a**, **1a·2b**, **1b·2a**, and **1b·2b**. NOEs shared by all four pairs are indicated by solid arrows. NOEs identified in some of the pairs are indicated by dashed arrows.

Table 1. Chemical Shift Data for α-Protons[a]

	Ala1	Ala2	Leu	Phe	Val	Gly1	Gly2
1a·2a	4.74		4.99	5.34	4.76	4.44	4.33
1a·2b	4.75	5.13		5.26	4.71	4.45	4.41
1c·2a	<4.70		<4.70	<4.70	<4.70	<4.70	<4.70
1c·2b	<4.80	<4.80		<4.80	<4.80	<4.80	<4.80
1a	4.60				4.57	4.30	
1c	4.64				4.48	4.54	
3 + 4a	5.04		4.61	4.82	4.66	4.25	3.99
3 + 4b	5.05	4.82		4.94	4.65		
4a			4.31	4.54			4.10
4b		4.53		4.67			3.93

[a] NMR (500 MHz) measurements were carried out at 4 mM of sample concentration in $CDCl_3$.

chains. The fact that no NOEs are observed between the hydrogens of the template segments and those of the tripeptide segments supports the expected, regiospecific registration of the single hybrid strands. The NOEs between protons *1* and *42*, and *21* and *22***,** further suggest that there is no fraying at even the two termini of these hybrid duplexes. Strong cross-strand NOEs in the peptide segments of each of the four duplexes are identified, which are consistent with the existence of *β*-sheet structures.

Results from NOESY studies on all four hybrid duplexes are consistent with the regiospecific registration of the single strands and the existence of antiparallel *β*-sheet segments.[29] The NOESY data (800 MHz, $CDCl_3$) based on duplex **1a·2a**, whose 1D spectrum shows the best resolved signals, are discussed here in detail. The most conclusive evidence for the existence of a *β*-sheet-like structure in the tripeptide segment of **1a·2a** involves the observation of numerous long-range, strong NOEs between residues of the two tripeptide chains. These NOE contacts include those between the backbone protons such as the strong cross-strand NH···NH interaction of the H-bonded amide pair (Ala···Phe). A strong interstrand Hα···Hα interaction is detected between the non-H-bonded pair (Val···Leu). Other strong cross-strand backbone interactions include those between protons *12* and *32*, *13* and *32*, *20* and *24*, and *21* and *22* (Figure 4a). Strong NOEs are also observed between the amino acid side chains Ala···Phe and Val···Leu, suggesting that the peptide chains are registered as expected (Figure 4b). In the same peptide chain, the absence of any adjacent, interresidue $N_iH\cdots N_{i+1}H$ NOEs and the observation that strong NOEs exist for $C_i^{\alpha}H\cdots N_{i+1}H$ (Figure 4c) provide additional support for an extended conformation for the peptide chains. These data are fully consistent with a structure consisting of extended, antiparallel peptide chains that are registered through hydrogen bonds.

To confirm that the duplex template is indeed responsible for the observed pairing of the tripeptide strands, a 1:1 mixture of hybrid strand **1a** and tripeptide **4a**, which is equivalent to removing one of the templates of duplex **1a·2a**, was examined by 2D NMR. The major NOEs are shown in Figure 5a. In contrast to **1a·2a** whose NOESY spectrum is consistent with a duplex with the expected registration of residues through H-bonding, the NOESY spectrum of mixture **1a** + **4a** reveals strong cross-strand NOEs that do not exist in the spectrum of **1a·2a**. The NOEs include those between protons *32* and *4*, *32* and *10*, *32* and *12*, and *29* and *7*. These cross-strand contacts indicate that in the absence of one of the template strands, the tripeptides cannot specifically associate with each other. Other noteworthy contacts are those between protons *7* and *21*, and *7* and *20*, indicating that some molecules of **1a** either adopt a folded conformation or the molecules self-associate in their tripeptide segments. NOESY study on a 1:1 mixture of **1a** and **3** revealed similar NOEs that indicate nonspecific cross-strand contacts (Figure 5b). Contacts between protons of the peptide terminus and the template in **1a** are also strong. Furthermore, NOEs corresponding to the self-association of **3** are clearly identified.

A 1:1 mixture of tripeptides **3** and **4a**, corresponding to removing both template strands in **1a·2a**, was examined by 2D NMR (NOESY, 500 MHz, 4 mM in $CDCl_3$). Cross-strand NOEs corresponding to all possible combinations of the tripeptides, i.e., self-association of **3** or **4a**, and association of **3** and **4a**, were observed (Figure 6). Qualitatively, NOEs corresponding to the self-association of **3** are the strongest; NOEs resulting from the contacts of **3** and **4a** are weaker, and the self-association of **4a** gives the weakest NOEs. Therefore the observed NOEs are not consistent with an alignment shown by

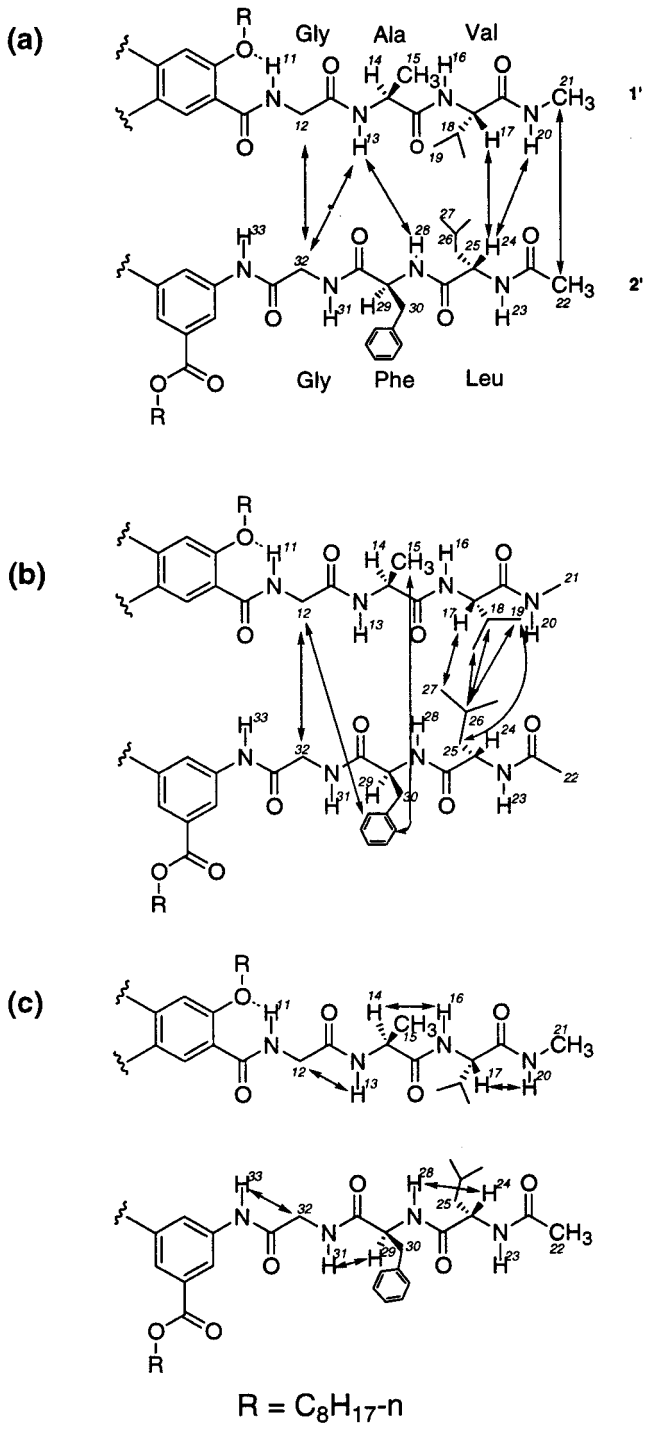

Figure 4. Long-range strong NOEs revealed by NOESY studies of **1a·2a** (800 MHz, mixing time 0.5 s, 4 mM in $CDCl_3$). (a) Backbone−backbone interactions. (b) Side chain−side chain interactions. (c) Interresidue $C_i^{\alpha}H\cdots N_{i+1}H$ interactions.

the tripeptide chains in **1a·2a**. Instead, these results are in agreement with a scenario involving random association of tripeptide chains through H-bonding and/or side-chain interactions. NOESY study on another 1:1 mixture of tripeptides **3** and **4b** revealed NOEs similar to those of **3** and **4a**.[29] Strong NOEs consistent with the self-association of tripeptide **3** were once again identified.

At the same concentration (4 mM), the behavior of duplexes **1a·2a**, **1a·2b**, **1b·2a**, and **1b·2b** is in contrast to that of the 1:1 mixtures of tripeptides **3** and **4a** or **3** and **4b**. The NOESY spectra of the hybrid duplexes show NOEs that only correspond to the specific pairing of the two different hybrid strands. NOEs corresponding to further association of the hybrid duplexes are not found in the NOESY spectra. Therefore the duplex template not only directs the specific pairing of the tripeptide chains, but also prevents the nonspecific association of peptide strands, which carry extra hydrogen bond donors and acceptors. The templates may have impeded the random association of the peptide segments because of (1) parallel alignment of duplexes through H-bonding interactions in the tripeptide region is prevented by the steric hindrance from the duplex template, (2) antiparallel alignment of the tripeptide region is interrupted due to the incorrect registration of H-bond donors and acceptors, which is cause by the presence of intramolecular H-bond between the NH group of one of the two Gly residues with the aryl ether O atom of the template (the S(6) type intramolecular H-bonds act to pre-organize[20,24] the template strands and, more importantly, to establish the hydrogen bonding pattern between the tripeptides), and (3) the significantly enhanced stability (see below) of the hybrid duplexes as compared to the presumed tripeptide dimers (or higher aggregates).

(3) Vapor Pressure Osmometry (VPO). The aggregation of the templates, tripeptides, and the hybrid strands was investigated by VPO measurements. The results are listed in Table 2. Template strand **1** (**2** had limited solubility) was monomeric and showed no self-aggregation. The template duplex **1·2** existed in solution as a heterodimer, as is evidenced by its aggregation number of ∼1. The hybrid single strand **1a** (**2a** had limited solubility) did not show any self-association. As expected, the hybrid duplex **1a·2a** had an aggregation number of 1 and thus should be a heterodimer. At 5 mM, tripeptide **4a** (**3** had limited solubility) showed almost no aggregation, which may be due to its weak self-association. An aggregation number of 1.4 was obtained for **4a** at a higher concentration of 10 mM. Surprisingly, a 1:1 mixture of **3** and **4a** gave an aggregation number of ∼1 at 4 mM of each tripeptide, indicating either the existence of a heterodimer or that there is an equilibrium between monomeric tripeptides and higher aggregates.

(4) ^{1}H NMR Binding Studies. The binding strength of **1·2**, the self-association of **4a**, and the association of **3** and **4a** were investigated by diluting the corresponding solutions and following the concentration-dependent changes of the chemical shifts of the amide protons that were involved in intermolecular H-bonding. For **1·2**, all four aniline NH signals showed similar concentration-dependent changes in their chemical shifts in $CDCl_3$ containing 5% DMSO-d_6, supporting their role in intermolecular H-bonding. Depending on the specific NH signal followed, nonlinear regression analysis[31] of the NMR data led to slightly different values of an association constant that was at the lower end of 10^3 M^{-1} for **1·2** (Table 3). Assuming a simple dimerization mode, similar analysis found that the self-association of tripeptide **4a** was very weak even in pure $CDCl_3$ (Table 3).

Although the limited solubility of tripeptide **3** did not allow the direct assessment of its self-association, a 1:1 mixture of **3**

(31) Wilcox, C. S. In *Frontiers in Supramolecular Organic Chemistry and Photochemistry;* Schneider, H.-J., Durr, H., Eds.; VCH: New York, 1991. The dimerization constant was obtained by fitting the NMR data into a modified dimerization equation with the program Kaleidagraph on a Macintosh computer.

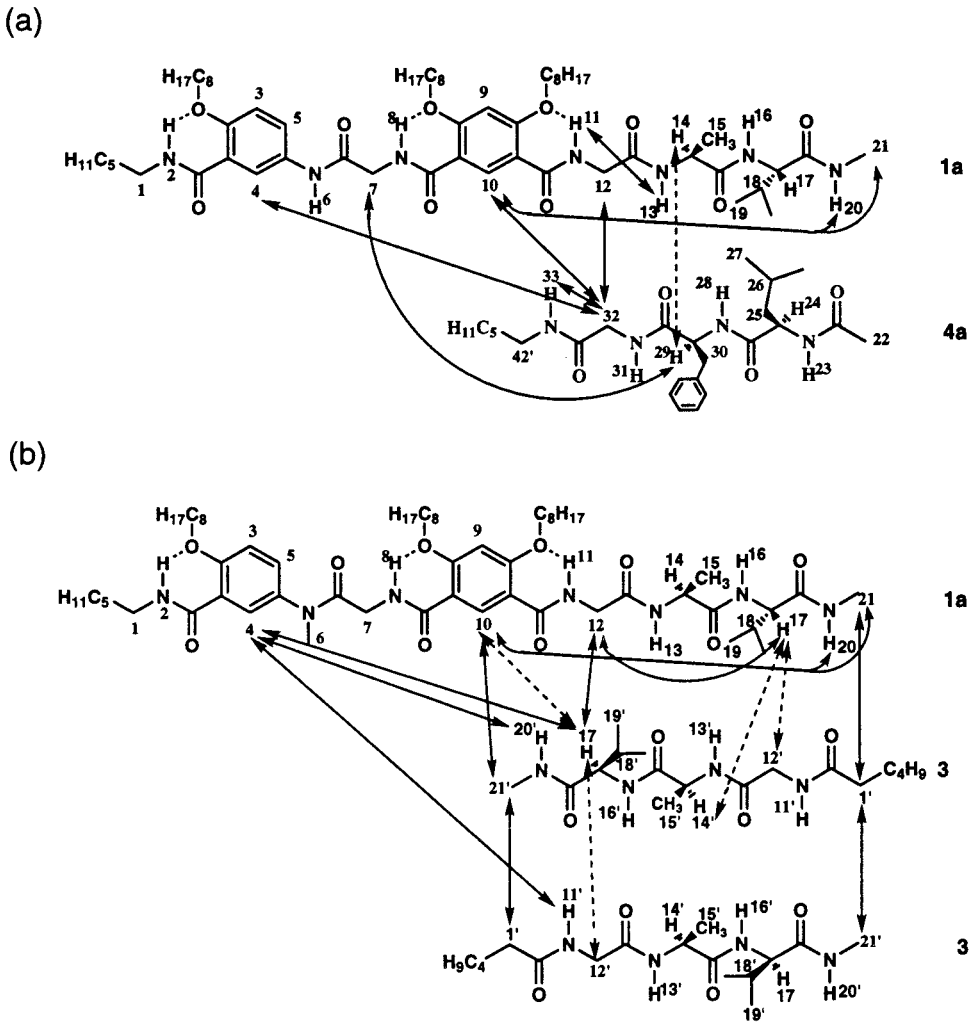

Figure 5. Summary of long-range NOEs (NOESY, 500 MHz, mixing time 0.5 s, 4 mM in $CDCl_3$) observed for the 1:1 mixtures of (a) **1a** + **4a**, and (b) **1a** + **3**.

and **4a** was quite soluble in chloroform. The association constant of **3** and **4a** was determined by diluting a solution in $CDCl_3$. Surprisingly, the resultant values varied significantly and fell into two different groups: (1) data based on the NH signals of **3** led to numbers in the 10^3 M^{-1} range and (2) data based on the NH signals of **4a** led to much smaller values in the 10^2 M^{-1} range. Such a result indicates the existence of a strong heterodimer consisting of **3** and **4a**, which requires that similar values of the association constant being obtained based on the NH signals of either strand is unlikely. Instead, the two sets of different values are consistent with a strong self-dimer (**3·3**) that interacts weakly with **3**, which is consistent with the conclusion from the above NOESY studies on **3**, **4a**, and **4b,** and can also explain the VPO result of the mixture of **3** and **4a**. In the presence of polar solvent such as DMSO, the association between **3** and **4a** and the self-association of **3** or **4** should be much weaker. However, analysis of the same (**3** + **4a**) mixture in $CDCl_3$ containing 5% DMSO-d_6 was not successful due to the precipitation of **3** out of this mixed solvent.

(5) Isothermal Titration Calorimetry. Determining the association constant of the hybrid duplex **1a·2a** in $CDCl_3$ or in $CDCl_3$/DMSO-d_6 turned out to be difficult due to the extensive overlap of numerous NH signals. Instead, titrations using isothermal titration calorimetry (ITC) were carried out. Titrating a solution of 1.1 mM of **1a** with 8.4 mM of **2a** in 5% DMSO/$CHCl_3$ gave an association constant of $(2.4 \pm 0.4) \times 10^4$ M^{-1}, along with $\Delta G = -5.9 \pm 0.1$ kcal/mol and $\Delta H = -3.9 \pm 0.3$ kcal/mol. The corresponding thermogram is shown in Figure 7. Under the same conditions, ITC titration failed to detect association between the template strands **1** and **2**, and between tripeptides **3** and **4a** in 5% DMSO/$CHCl_3$. Therefore the addition of the tripeptide strands to **1** and **2** led to a hybrid duplex with enhanced stability. Such an increase in stability may very likely be due to the cooperative interaction between the duplex template and the tripeptide segment. However, probing the energetic nature of duplex **1a·2a** by using differential scanning calorimetry (DSC) was not feasible due to the low boiling points of the solvents ($CHCl_3$ and CH_2Cl_2) that were required for solubilizing this duplex.

Conclusion

Our study shows that the noncovalent template based on a hydrogen-bonded duplex is highly directional and specific in effecting the assembly of two different structural fragments. The resulted hybrid duplexes adopt a well-defined conformation in solution. A two-stranded, β-sheet conformation is formed, as revealed by the changes in H_α chemical shifts, the numerous inter- and intrastrand NOEs, the VPO results, and the enhanced

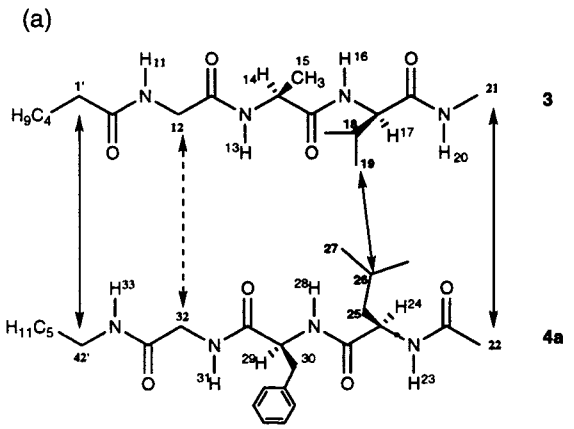

Can not be unequivocally distinguished from **b** due to signal overlap which prevent the observation of NOE between protons 17 and 24.

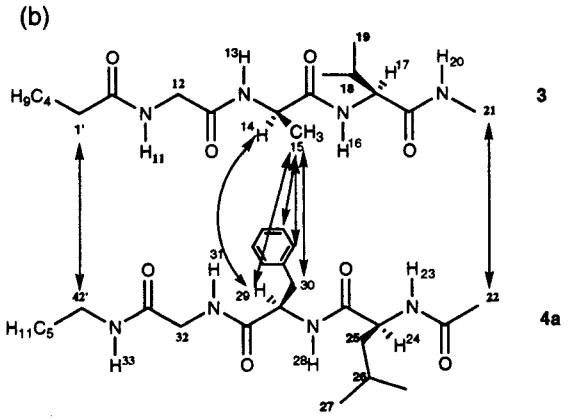

The existence of this pattern is supported by the strong NOE between protons 14 and 29.

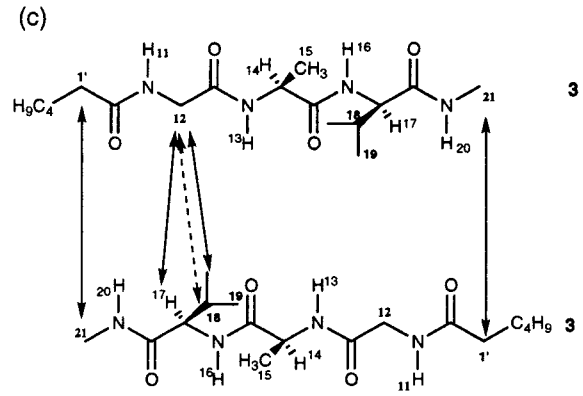

The strong NOEs between 12 and 17 support this pattern.

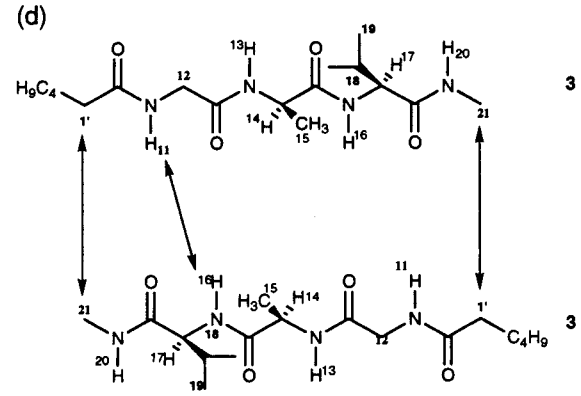

The strong NOE between 11 and 16 support this pattern.

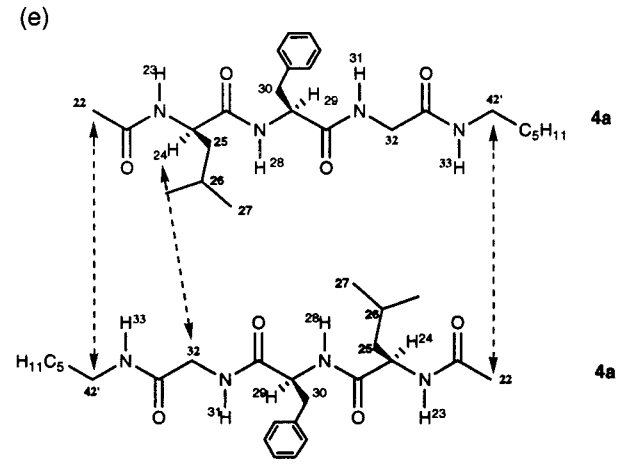

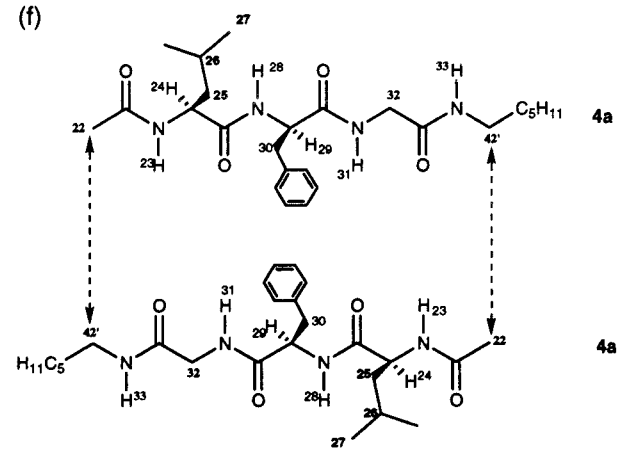

The weak NOEs consistent with the above patterns suggest that the self-association of **4a** is much weaker than the association between **3** and **4a** and the self-association of **3**.

Figure 6. Summary of long-range NOEs (NOESY, 500 MHz, mixing time 0.5 s, 4 mM in $CDCl_3$) observed for the 1:1 mixtures of **3** and **4a**. Strong contacts are indicated by solid arrows; weak contacts are represented by dashed arrows.

stability of the hybrid duplex **1a·2a**. This noncovalent approach has turned an otherwise intramolecular process, i.e., β-hairpin (or two-stranded β-sheet) formation, into an intermolecular one, which should facilitate detailed thermodynamic studies in the future. Given the facility in programming the H-bonded duplexes, a template-based, noncovalent combinatorial approach should provide numerous β-sheet structures, which not only will lead to invaluable insight into the factors affecting β-sheet formation, but also should provide a platform for generating covalently linked β-sheet structures based on an assembly-crosslinking strategy. The assembly of multiple peptide strands can also be envisioned. For example, template-directed assembly of two β-hairpins should lead to four-stranded β-sheets. The design of duplex templates with various side chains that are

Table 2. Concentrations and Aggregation Numbers (VPO) in Chloroform[a,b]

substrate	concn (mmolar)	concn (mmolal)	aggregation no.
1	4.1	2.8	0.9 ± 0.1
1 + **2**	4.6	3.2	0.9 ± 0.1
4a	4.9	3.3	1.1 ± 0.1
3 + **4a**	4.0	2.7	1.0 ± 0.1
1a	4.3	2.9	1.0 ± 0.1
1a + **2a**	4.9	3.3	1.0 ± 0.1

[a] Aggregation number of GFL at 10 mM is 1.4 ± 0.1. For **1** + **2**, **3** + **4a**, or **1a** + **2a**, the two components have identical concentration with the shown value. Some of the data may be 0.9 or 1.1 because of the 10% experimental error in this type of measurement. [b] Plus/minus values are reported at the 95% confidence level.

Table 3. Association Constants from NMR Binding Studies[a]

1·**2**[b]		**4a**[c]	
data based on	K_a (M^{-1})	data based on	K_a (M^{-1})
H41	$(0.67 \pm 0.10) \times 10^3$	H23	14.5 ± 2.5
H6	$(1.25 \pm 0.24) \times 10^3$	H28	22.6 ± 3.2
H36	$(1.14 \pm 0.12) \times 10^3$	H31	8.4 ± 1.9
H33	$(0.36 \pm 0.04) \times 10^3$	H33	18.3 ± 2.8

3 + **4a**[d]			
data based on N*H* of **3**		data based on N*H* of **4a**	
H11	$(0.92 \pm 0.18) \times 10^3$	H23	150 ± 14
H13	$(1.91 \pm 0.63) \times 10^3$	H28	190 ± 14
H16	$(0.58 \pm 0.14) \times 10^3$	H31	110 ± 13
H20	$(1.90 \pm 0.60) \times 10^3$	H33	167 ± 20

[a] See Figure 3 for atom labeling. [b] NMR measurements were carried out from 64 to 0.125 mM of each of the two strands in 5% DMSO-d_6/$CDCl_3$. [c] NMR measurements were carried out from 51.2 to 0.1 mM in $CDCl_3$. A dimerization mode is assumed when fitting data. [d] NMR measurements were carried out from 25.6 to 0.1 mM in $CDCl_3$. A dimerization mode is assumed when fitting data.

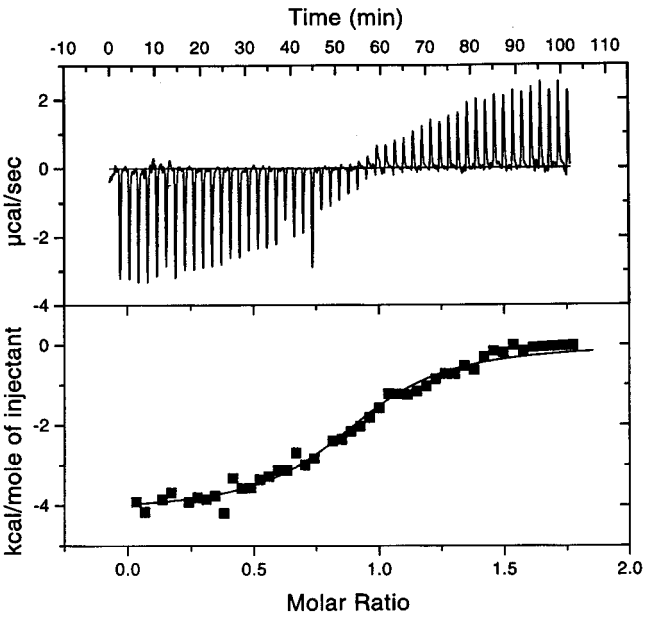

Figure 7. Calorimetry binding isotherm for the titration of **1a** with **2a** in 5% DMSO/chloroform.

compatible to a variety of solvents is being pursued. The resultant duplexes will facilitate characterization based on techniques such as DSC and far-UV circular dichroism that could not be employed here due to the limit of the solvents involved. The generality of our approach is demonstrated by the existence of β-sheet structures in all four hybrid duplexes containing different amino acid residues. This, combined with the convenience of simply mixing templated peptide strands into duplexes, distinguishes our system from existing, covalent templating strategies. The specificity of a water-soluble duplex template, in combination with the stability of peptide strands that contain hydrophobic clusters,[9] may lead to the specific assembly of sheet-like structures that are stable in an aqueous environment. The corresponding results will be reported in due course.

Experimental Section

General Methods. All chemicals were purchased from Aldrich, Fluka, and Sigma and used as received unless otherwise noted. The organic phase from all liquid extractions was dried over Na_2SO_4 unless specified otherwise. All products were detected as single spots by thin-layer chromatography (precoated 0.25 mm silica plates from Aldrich). All samples were purified either by recrystallization or by flash column chromatography and dried completely under high vacuum before characterized by ^{1}H NMR (400 M), ^{13}C NMR (100 M), and elemental analysis. All ^{1}H NMR and ^{13}C NMR spectra were recorded on a Varian VXR 400 spectrometer (400 M). NMR chemical shifts were reported in ppm relative to TMS. All *J* values are reported in hertz. NOE measurements were performed with the steady-state NOEDIF protocol on degassed samples. The synthesis of **a**, **1p**, **1v**, **2c**, and **2f** was reported previously by us.[22,23]

Vapor-Pressure Osmometry. The aggregation numbers for the peptide, template, and peptide−template strands were determined by employing a Wescor 5500-XR vapor pressure osmometer operating at 37 °C. Known concentrations of the individual strands or the complementary duplexes were prepared in chloroform. Calibration curves of VPO reading vs molality were obtained by employing biphenyl as the calibration standard. A least-squares analysis of 10 points provided a correlation coefficient of 0.991. Solutions of the individual strands of the complementary strands were placed in the osmometer and the instrument reading was converted into concentration by using the calibration curve. Each VPO datum was generated by making three independent solutions of each strand at the same concentration and measuring each solution a minimum of four times.

Binding Studies. The binding parameters were determined by titrating a 1.1 mM solution of **1a** with 8.4 mM **2a** in 5% DMSO/$CHCl_3$ in an Omega isothermal titration calorimeter (MicroCal, Northampton, MA). The cell was thermostated to ±0.1 °C with use of a circulating bath. All of the experiments were performed at 25 °C. The enthalpy of binding between the two strands was determined from heats of multiple single injections. Injection volumes were 5 μL, with 3 min of equilibration time allowed between injections. The heat of dilution of **2a** into 5% DMSO/$CHCl_3$ solvent was determined and the *host*−*guest* titration heat was adjusted by this contribution.

The binding constants, *K*, and the number of binding sites, *n*, were extracted from the calorimetric data employing the Origin data analysis software supplied with the Omega titration calorimeter. A complete description of the data analysis has been published by Brandts and coworkers.[32]

NMR dilution experiments were performed at 25 °C. The solution of a sample was diluted and the chemical shifts of the NH-protons were followed in the ^{1}H NMR spectra and analyzed on the basis of an equation described before.[31]

Supporting Information Available: NMR spectra and experimental details (PDF). This material is available free of charge via the Internet at http://pubs.acs.org.

JA010701B

(32) Wiseman, T.; Williston, S.; Brandts, J. F.; Lin, L.-N. *Anal. Biochem.* **1989**, *179*, 131.